

Interplay of Ligand Chirality and Metal Configuration in Mononuclear Complexes and in a Coordination Polymer of Cr(III)[†]

Ai Wang,^a Carina Merkens,^a and Ulli Englert^{*a}

Received Xth XXXXXXXXXXXX 20XX, Accepted Xth XXXXXXXXXXXX 20XX

First published on the web Xth XXXXXXXXXXXX 200X

DOI: 10.1039/b000000x

Electronic Supplementary Information

^a Institute of Inorganic Chemistry, RWTH Aachen University, Aachen, Germany. Fax: +49-241-8092288; Tel: +49-241-8094666; E-mail: ullrich.englert@ac.rwth-aachen.de

List of Figures

S1	Ball and stick model of the asymmetric unit in 1	7
S2	Displacement ellipsoid plot (50 % probability) of the asymmetric unit in 1	7
S3	Ball and stick model of the asymmetric unit in 2	8
S4	Displacement ellipsoid plot (50 % probability) of the asymmetric unit in 2	8
S5	Ball and stick model of the asymmetric unit in 3	9
S6	Displacement ellipsoid plot (50 % probability) of the asymmetric unit in 3	9
S7	Ball and stick model of the asymmetric unit in 4	10
S8	Displacement ellipsoid plot (50 % probability) of the asymmetric unit in 4	10
S9	Ball and stick model of the asymmetric unit in 6	11
S10	Displacement ellipsoid plot (50 % probability) of the asymmetric unit in 6	11
S11	The disordered model of nitrate ions and water molecules in 6	11
S12	Ball and stick model of the asymmetric unit in 7	12
S13	Displacement ellipsoid plot (50 % probability) of the asymmetric unit in 7	12
S14	Ball and stick model of the asymmetric unit in 8 . Disordered water molecules with site occupancy < 0.5 have been omitted.	13
S15	Displacement ellipsoid plot (50 % probability) of the asymmetric unit in 8 , excluding part of disordered water molecules.	13
S16	Experimental (Exp) and simulated (Sim) powder diffraction pattern of 1	14
S17	Experimental (Exp) and simulated (Sim) powder diffraction pattern of 2	14
S18	Experimental (Exp) and simulated (Sim) powder diffraction pattern of 4	15
S19	Two experimental powder diffraction patterns of 5 showing the same solid is obtained reproducibly.	16
S20	Experimental (Exp) and simulated (Sim) powder diffraction pattern of 6	16
S21	Simulated (Sim) powder diffraction pattern of 7 based on the single crystal diffraction experiment and two successive experimental powder patterns. Exp1 what obtained after 5 min; diffraction intensities are mostly due to a desolvated product of unknown structure, the regions highlighted in green show residual diffraction intensity due to the original solvate. Exp2 exclusively corresponds to desolvated product.	17
S22	Experimental (Exp) and simulated (Sim) powder diffraction pattern of 8	17

1 Crystallization, structure solution and refinement of 1 - 4 and 6 - 8

All solids contain the *R,R*-enantiomer of the chiral ligand *R,R*-1,2-diaminocyclohexane. In all cases the assigned stereochemistry was confirmed by refinement of the Flack parameter.¹

1.1

Red plate-shaped crystals of **1** were obtained from DMSO by evaporating the solvent at room temperature. **1** crystallizes in the monoclinic space group $P2_1$ with two $[\text{Cr}(\text{R,R-chxn})_2(\text{DMSO})\text{Cl}]^{2+}$ cations in Δ configuration, four uncoordinated Cl^- anions and two disordered DMSO molecules (Figs. S1 and S2). During refinement, rigid bond and similarity restraints were used for the displacement parameters of sulfur and carbon atoms of the uncoordinated DMSO molecules. Two rigid-bond restraints with effective standard deviation 0.01 Å were applied.

1.2

Purple block-shaped single crystals of **2** suitable for diffraction experiments were obtained from EtOH by evaporation at ambient temperature. **2** crystallizes in the monoclinic space group $C2$; the asymmetric unit contains two $[\text{Cr}(\text{R,R-chxn})_2\text{Cl}_2]^+$ cations (one in Δ and one in Λ configuration) two Cl^- anions located between two cations, and two EtOH molecules (Figs. S3 and S4). These EtOH molecules are disordered about a crystallographic twofold axis. In total, 33 restraints were employed in the final refinement.

1.3

After recrystallization from water, individual orange rod-shaped crystals of **3** can be distinguished from those of the majority solid **4**. The compound adopts the monoclinic space group $P2_1$ with one $[\text{Cr}(\text{acacCN})(\text{R,R-chxn})_2]^{2+}$ cation and two NO_3^- anions in the asymmetric unit (Figs. S5 and S6). In the nitrate associated with N7, the nitrogen and two of the oxygen atoms are disordered over two alternative positions with occupancies 0.673(9) and 0.327(9). Similarity restraints were used to ensure chemically reasonable distances in this disordered moiety.

1.4

4 was obtained at ambient temperature as a phase pure product starting from **2** under retention of the metal configuration; suitable yellow block-shaped single crystals can be grown from water by evaporation at room temperature. The asymmetric unit in the triclinic space group $P1$ comprises the whole unit cell and contains two $[\text{Cr}(\text{acacCN})(\text{R,R-chxn})_2]^{2+}$ cations, one in either configuration, four nitrate anions and one water molecule (Figs. S7 and S8). One NO_3^- is disordered over two alternative positions with occupancies 0.694(10) and 0.306(10). Similarity and coplanarity restraints were used to ensure chemically reasonable geometries in the disordered moiety.

1.5

Red block-shaped crystals **6** crystallized from water. The compound adopts the triclinic space group $P1$, with four symmetrically independent $[\text{Cr}(\text{acacCN})_2(\text{R,R-chxn})]^+$ cations, NO_3^- anions and water molecules in the unit cell (Figs. S9 and S10). Δ and Λ configured cations occur in a 2:2 ratio. The disorder involving a nitrate and a water moiety in two alternative orientations is explained in Fig. S11: one orientation of these residues is associated with N20, O26A, O27A, O28 of the NO_3^- and O4W of the H_2O , the alternative orientation with N21, O26B, O27B, O29 and O5W. The sum of the site occupancies for these atoms was constrained to unity; refinement converged for almost equal values of 0.507(7) and 0.493(7). Hydrogen atoms in this disordered water molecule were calculated to match the closest $\text{O}\cdots\text{H}\cdots\text{O}$ contacts.

1.6

Suitable red block-shaped single crystals of **7** were grown from methanol by evaporation. The compound crystallizes in the monoclinic space group $P2_12_12_1$, with one $[\text{Cr}(\text{acacCN})_2(\text{R,R-chxn})]^+$ cation, a well-ordered PF_6^- anion and a MeOH molecules in the asymmetric unit (Figs. S12 and S13).

1.7

Crystals of **8** belong to the monoclinic space group *C222*. The Ag cation occupies Wyckoff position 2a and hence adopts crystallographic D_2 symmetry. Two Cr cations per Ag are located on a twofold axis in Wyckoff position 4h; the twofold axis passes through the Cr and the chxn ligand. One of the hexafluorophosphate counter anions is situated in position 2b, the other in 4h. The latter moiety is disordered; the occupancy sum for the alternative orientations was constrained to unity, and distance restraints were used to ensure chemically reasonable geometry for this PF_6^- group. Several alternative and in part mutually exclusive sites of fractional occupancy for solvent water molecules were identified in the voids between cationic framework and counter anions, and two alternative strategies were followed to treat this area of disordered solvent: a) in a first approach, the BYPASS algorithm² as coded in PLATON³ indicated a void volume of 620 Å³ and an electron count of 168 e per unit cell. Tentative refinement of the non-solvent part of the structure after correction for the diffuse solvent contribution resulted in acceptable agreement factors (wR_2 ca 0.15) but unsatisfactory displacement parameters of two atoms in the hexafluorophosphate counter anions. b) in a second model, seven discrete local maxima of residual electron density were refined as water oxygen sites of partial occupancy. In agreement with the electron count from the first approach (ca 16 water molecules per unit cell, i. e. ca 2 water molecules per asymmetric unit) the sum of their occupancies was restrained to 2, and those sites with occupancies < 0.5 were assigned a common isotropic displacement parameter. No attempt was made to assign hydrogen atoms for the disordered solvent water molecules. This second structure model resulted in a higher target agreement factor (wR_2 ca 0.17) but more convincing anisotropic displacement parameters for the non-solvent part of the structure. The structural information reported here, in Table 3 and in the CIF, refers to this discrete site model for the solvent water molecules.

2 References

- [1] Flack H. D. Chiral and achiral crystal structures. *Helv Chim Acta.*, 2003, **86**, 905-921.
- [2] Van der Sluis, P. V. and Spek, A. L. *Acta Crystallogr. Sect. A:*, 1990, **46**, 194-201.
- [3] Spek A. L. *Acta Crystallogr. Sect. D:*, 2009, **65**, 148-155.

Table S1 Classical hydrogen bonds (Å, °) of **1**, **2**, **6** and **8**

Comp.	D-H...A	D-H	H...A	D...A	∠D-H...A	Symmetry-for-A	
1	N1-H1D...Cl3	0.98(3)	2.29(3)	3.231(4)	160(3)		
	N1-H1E...Cl4	0.99(3)	2.40(3)	3.258(4)	146(3)		
	N2-H2D...O4	0.98(3)	1.99(3)	2.915(5)	159(4)	x,-1+y,z	
	N2-H2E...Cl3	0.98(4)	2.30(3)	3.181(4)	149(3)	1-x,-1/2+y,2-z	
	N3-H3D...Cl3	0.98(2)	2.30(2)	3.241(4)	161(3)		
	N3-H3E...Cl3	0.97(3)	2.35(4)	3.220(4)	148(3)	1-x,-1/2+y,2-z	
	N4-H4D...Cl4	0.98(3)	2.34(3)	3.309(4)	171(3)	2-x,-1/2+y,2-z	
	N4-H4E...Cl4	0.98(3)	2.38(3)	3.299(4)	157(3)		
	N5-H5D...Cl5	0.98(3)	2.32(2)	3.254(4)	159(3)		
	N5-H5E...Cl5	0.99(3)	2.27(4)	3.172(4)	151(3)	2-x,-1/2+y,1-z	
	N6-H6D...Cl6	0.98(3)	2.39(3)	3.360(4)	171(3)	1-x,1/2+y,1-z	
	N6-H6E...Cl6	0.98(3)	2.36(3)	3.299(4)	159(3)	x,1+y,z	
	N7-H7D...O3	0.99(3)	2.01(3)	2.977(5)	166(3)	2-x,1/2+y,2-z	
	N7-H7E...Cl5	0.98(4)	2.32(4)	3.222(4)	153(3)	2-x,-1/2+y,1-z	
	N8-H8D...Cl5	0.99(4)	2.26(4)	3.238(4)	171(3)		
	N8-H8E...Cl6	0.98(3)	2.41(3)	3.306(4)	152(3)	x,1+y,z	
	2	N1-H1D...Cl2	0.98(8)	2.68(10)	3.112(11)	107(7)	
		N1-H1E...Cl3	0.99(9)	2.58(9)	3.528(11)	160(6)	
N2-H2D...Cl3		0.99(10)	2.31(10)	3.235(12)	155(8)	3/2-x,-1/2+y,1-z	
N2-H2E...O2		0.98(7)	2.13(10)	2.99(3)	146(7)	1/2+x,-1/2+y,z	
N3-H3D...Cl1		0.98(6)	2.55(7)	3.091(11)	114(7)	1/2+x,-1/2+y,z	
N3-H3D...Cl3		0.98(6)	2.64(8)	3.280(11)	123(6)	3/2-x,-1/2+y,1-z	
N3-H3E...Cl1		0.98(6)	2.41(6)	3.360(10)	163(6)	3/2-x,1/2+y,1-z	
N4-H4D...Cl6		0.98(7)	2.30(8)	3.253(11)	165(9)		
N4-H4E...Cl5		0.98(7)	2.39(8)	3.284(11)	150(7)	x,-1+y,z	
N5-H5D...Cl6		0.99(8)	2.39(8)	3.347(11)	163(7)		
N5-H5E...Cl3		0.99(7)	2.62(5)	3.417(11)	137(7)		
N6-H6D...O1		0.99(7)	2.14(8)	3.060(2)	154(7)	1/2+x,1/2+y,1+z	
N6-H6E...Cl6		0.99(9)	2.25(8)	3.222(11)	166(7)	3/2-x,1/2+y,2-z	
N7-H7D...Cl1		0.98(5)	2.67(9)	3.244(10)	118(7)	x,1+y,z	
N7-H7E...Cl3		0.99(8)	2.31(8)	3.182(11)	146(6)		
N8-H8D...Cl5		0.99(4)	2.45(6)	3.315(11)	146(7)	3/2-x,-1/2+y,2-z	
N8-H8E...Cl6		0.99(8)	2.54(7)	3.374(11)	141(8)	3/2-x,1/2+y,2-z	
6		O1W-H1W1...O23	0.89(5)	2.55(5)	3.132(6)	125(4)	
	O1W-H1W1...O25	0.89(5)	2.03(5)	2.913(6)	173(4)		
	O1W-H1W2...N10	0.87(4)	2.45(5)	3.248(5)	153(5)		
	O2W-H2W1...O17	0.85(4)	2.05(4)	2.864(6)	162(5)	1+x,y,z	
	N3-H3D...O1W	0.99(3)	2.18(3)	3.142(6)	166(3)		
	N3-H3E...O2W	0.98(2)	2.25(3)	3.083(6)	143(3)	x,y,1+z	
	O2W-H2W2...O24	0.88(6)	2.30(6)	3.085(7)	149(5)	1+x,y,-1+z	
	N4-H4D...O25	0.97(3)	2.24(3)	3.177(6)	161(3)	1+x,y,z	
	N4-H4E...N6	0.97(3)	2.21(3)	3.069(6)	146(3)	x,1+y,z	
	O3W-H3W1...O21	0.85	2.02	2.873(7)	180		
	O3W-H3W2...O5W	0.94	2.27	3.185(11)	164		

	N7-H7D...O3W	0.97(4)	2.09(4)	3.016(7)	158(3)	
	N7-H7E...O26B	0.97(3)	1.91(3)	2.824(8)	155(5)	1+x,y,z
	N7-H7E...O29	0.97(3)	2.50(4)	3.367(11)	148(4)	1+x,y,z
	N8-H8D...N2	0.98(3)	2.13(3)	3.101(6)	174(3)	1+x,y,z
	N8-H8E...O27B	0.99(3)	2.53(3)	3.240(10)	129(3)	
	N8-H8E...N5	0.99(3)	2.41(3)	3.235(5)	140(3)	1+x,y,z
	O5W-H5W1...O26B	0.85	2.39	2.940(12)	123	
	O5W-H5W1...O27B	0.85	2.02	2.875(14)	180	
	O5W-H5W2...O26B	0.85	2.40	2.940(12)	122	
	N11-H11D...O24	0.99(3)	2.21(4)	3.112(6)	150(4)	x,1+y,z
	N11-H11E...O17	0.99(3)	2.08(3)	3.040(6)	164(3)	x,1+y,1+z
	N11-H11E...O18	0.99(3)	2.29(4)	3.087(5)	137(3)	x,1+y,1+z
	N12-H12D...O20	0.99(1)	2.04(2)	3.021(5)	174(3)	x,1+y,1+z
	N12-H12E...O19	0.97(3)	2.07(3)	2.894(6)	141(3)	1+x,1+y,1+z
	N15-H15D...O20	0.98(4)	2.00(4)	2.975(5)	171(3)	1+x,y,z
	N15-H15E...O5W	0.98(3)	1.97(3)	2.879(9)	154(4)	1+x,y,z
	N16-H16D...O22	0.96(4)	2.29(4)	3.010(6)	131(3)	
	N16-H16E...O18	0.98(4)	2.13(3)	2.993(5)	146(4)	
8	N1-H1E...F1	0.99(2)	2.35(5)	3.189(8)	143(5)	
	N1-H1E...F2	0.99(2)	2.40(4)	3.281(12)	149(6)	

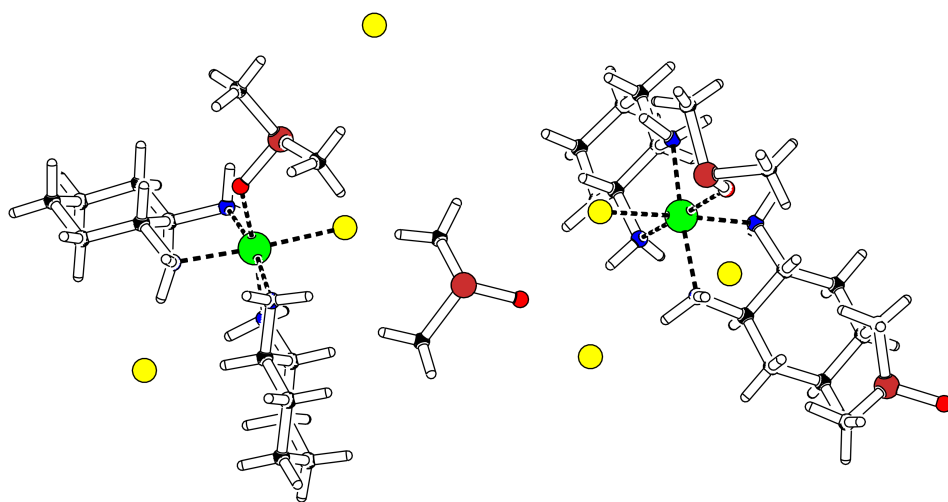


Fig. S1 Ball and stick model of the asymmetric unit in **1**.

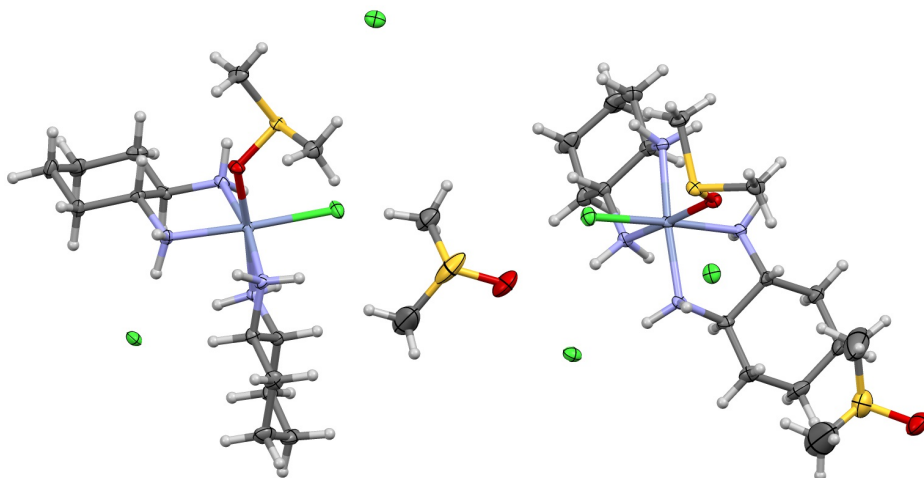


Fig. S2 Displacement ellipsoid plot (50 % probability) of the asymmetric unit in **1**.

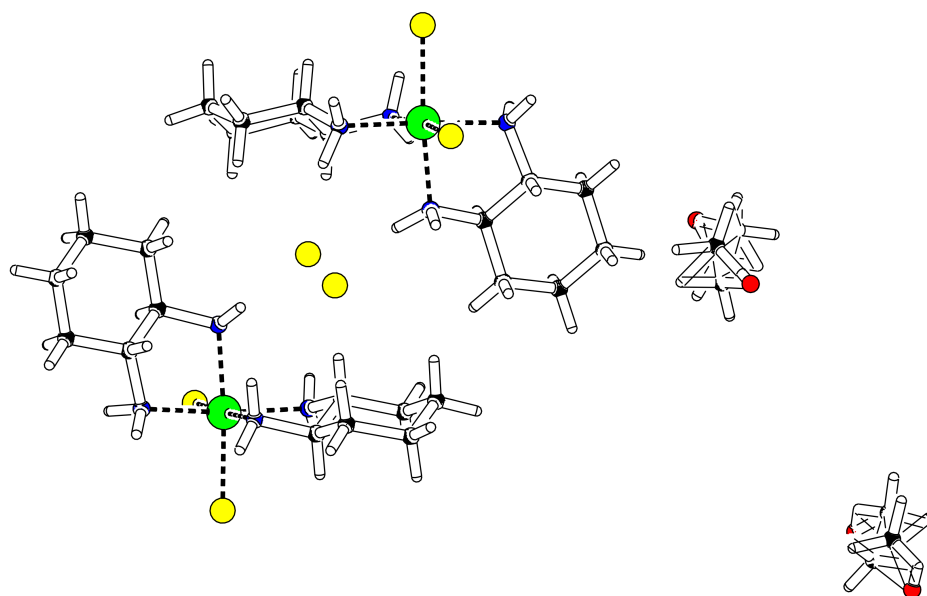


Fig. S3 Ball and stick model of the asymmetric unit in **2**.

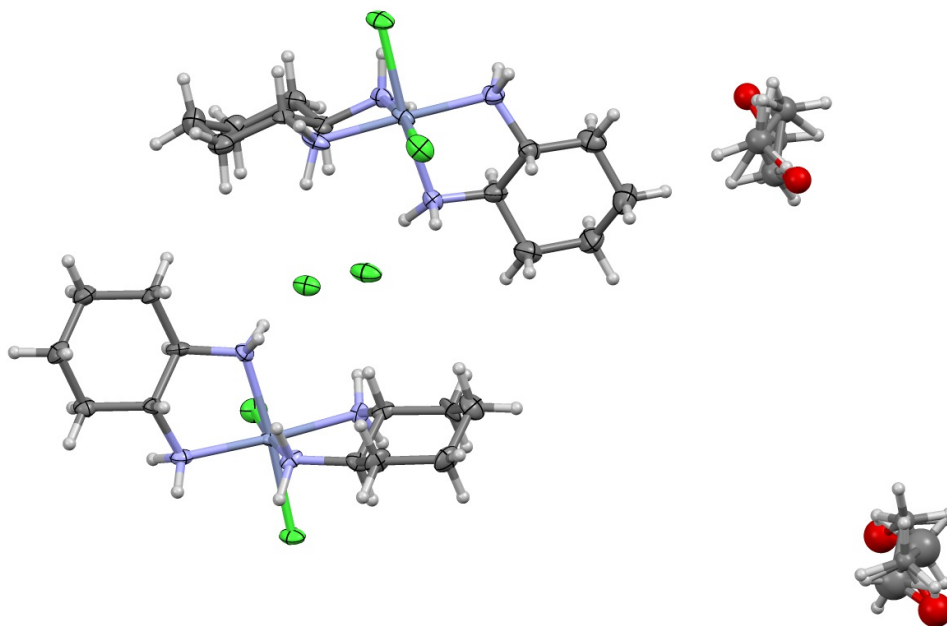


Fig. S4 Displacement ellipsoid plot (50 % probability) of the asymmetric unit in **2**.

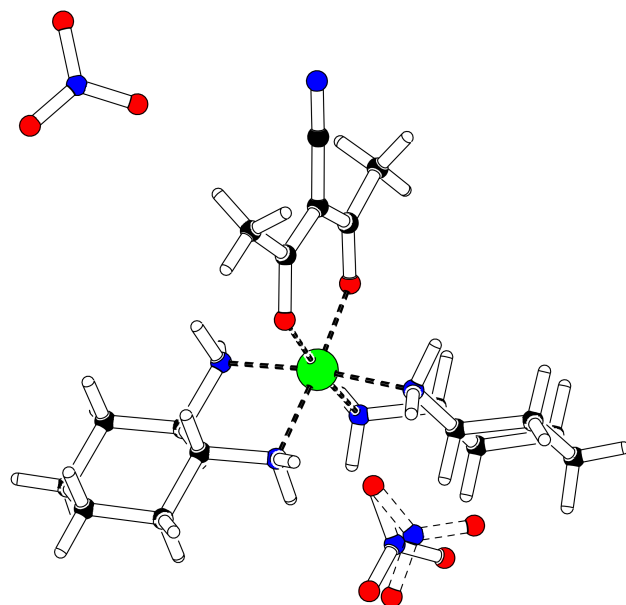


Fig. S5 Ball and stick model of the asymmetric unit in **3**.

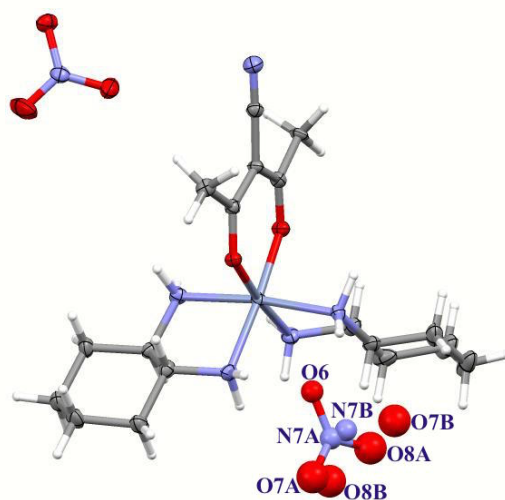


Fig. S6 Displacement ellipsoid plot (50 % probability) of the asymmetric unit in **3**.

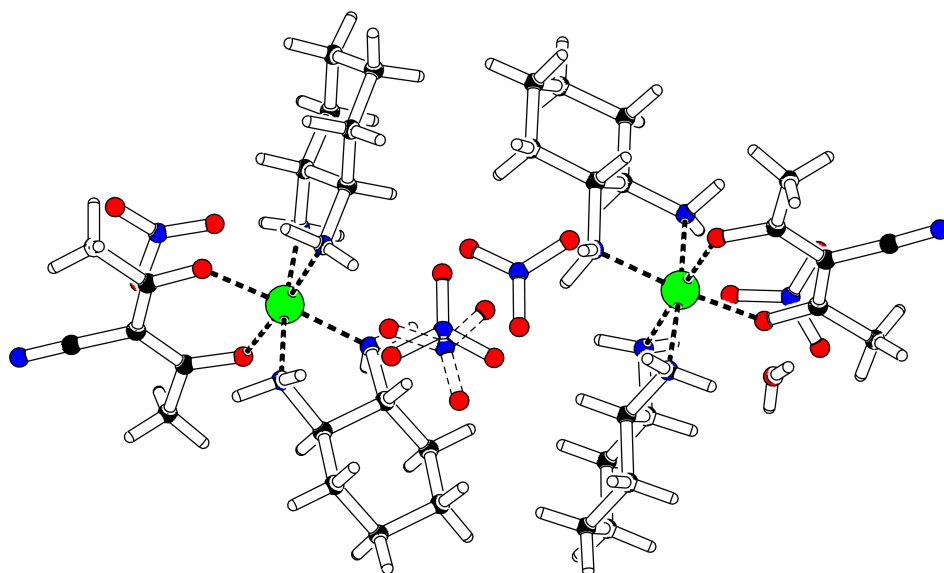


Fig. S7 Ball and stick model of the asymmetric unit in **4**.

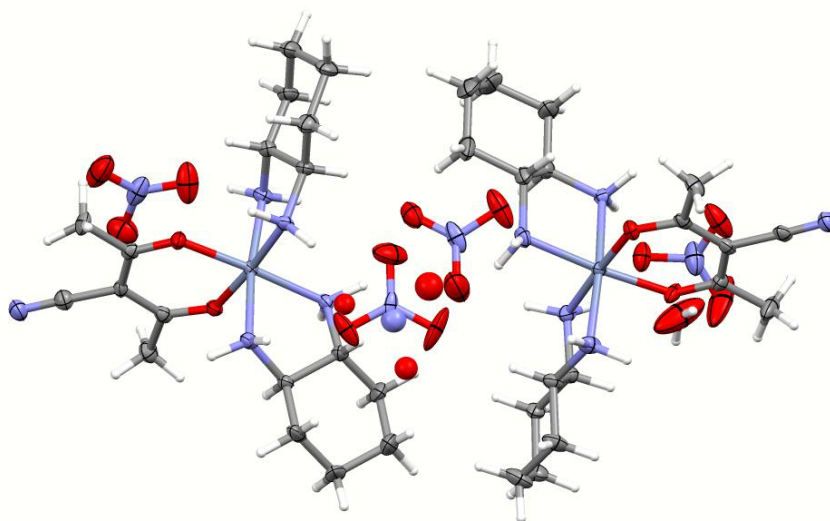


Fig. S8 Displacement ellipsoid plot (50 % probability) of the asymmetric unit in **4**.

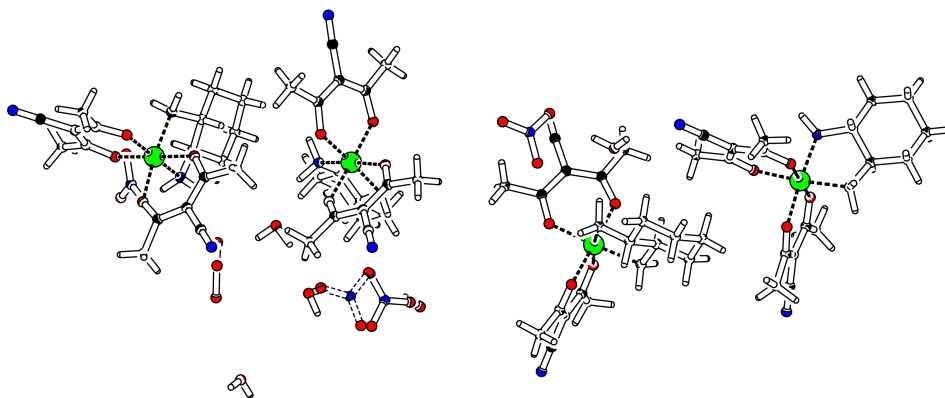


Fig. S9 Ball and stick model of the asymmetric unit in **6**.

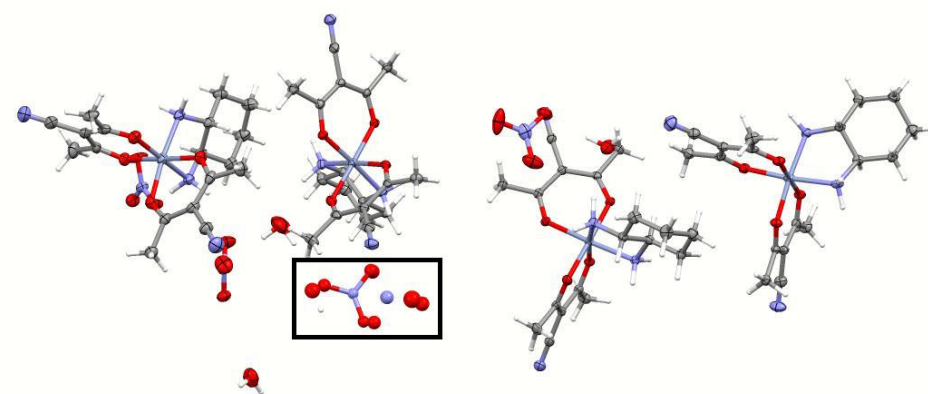


Fig. S10 Displacement ellipsoid plot (50 % probability) of the asymmetric unit in **6**.

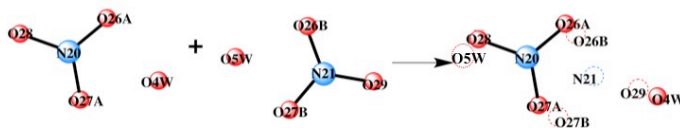


Fig. S11 The disordered model of nitrate ions and water molecules in **6**.

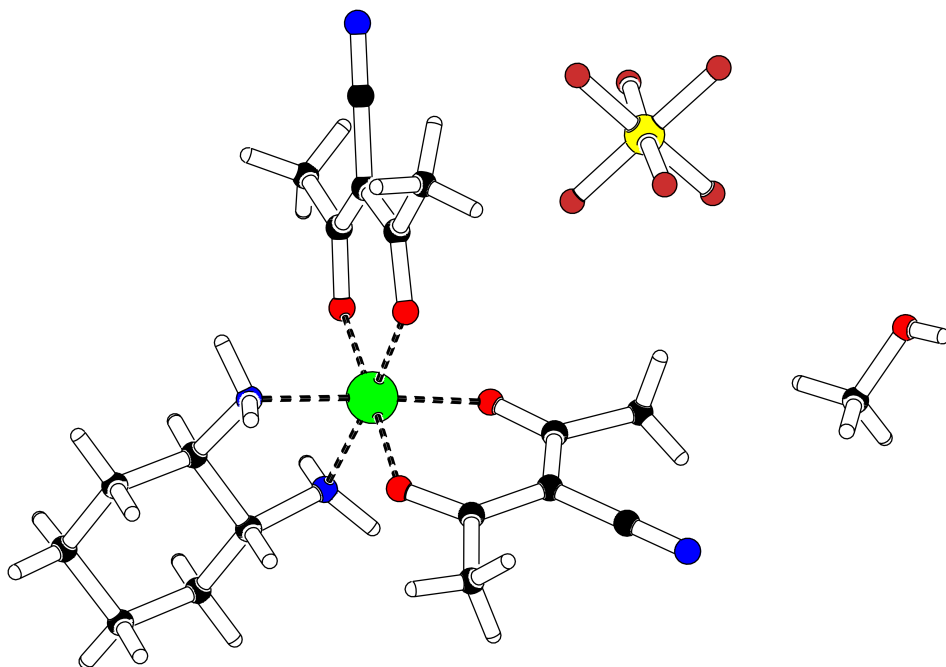


Fig. S12 Ball and stick model of the asymmetric unit in 7.

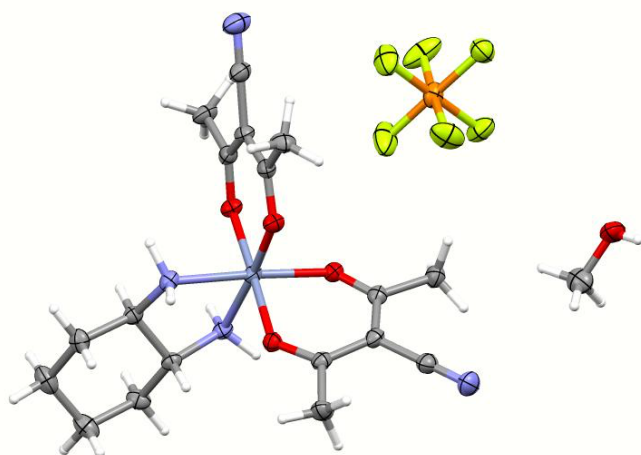


Fig. S13 Displacement ellipsoid plot (50 % probability) of the asymmetric unit in 7.

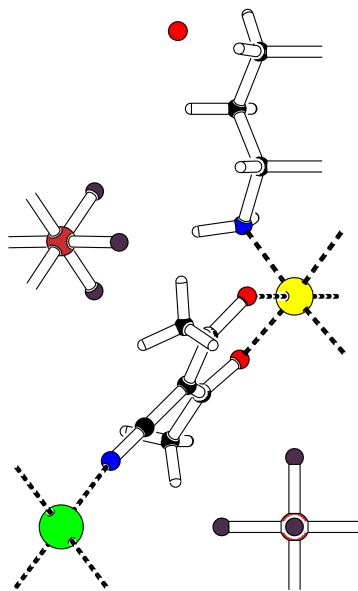


Fig. S14 Ball and stick model of the asymmetric unit in **8**. Disordered water molecules with site occupancy < 0.5 have been omitted.

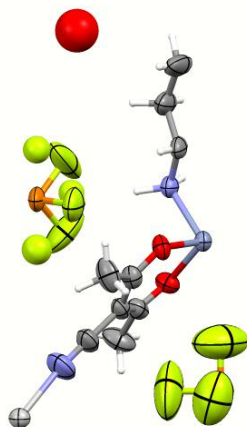


Fig. S15 Displacement ellipsoid plot (50 % probability) of the asymmetric unit in **8**, excluding part of disordered water molecules.

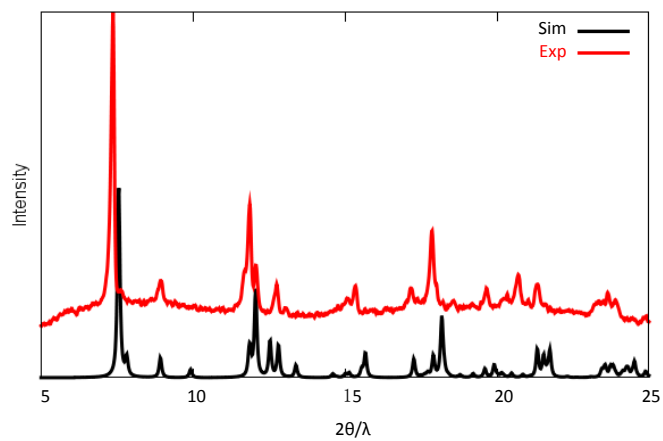


Fig. S16 Experimental (Exp) and simulated (Sim) powder diffraction pattern of **1**.

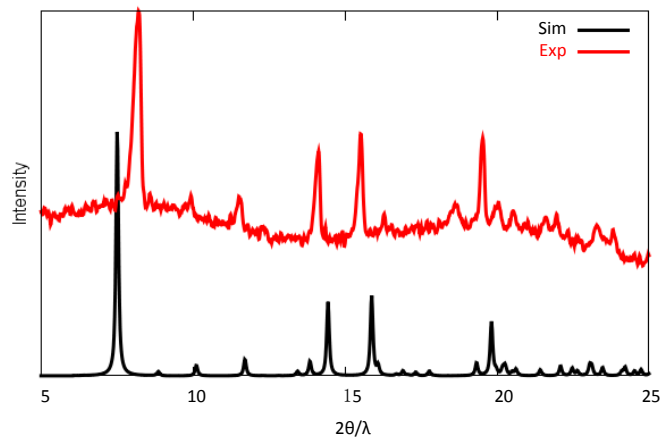


Fig. S17 Experimental (Exp) and simulated (Sim) powder diffraction pattern of **2**.

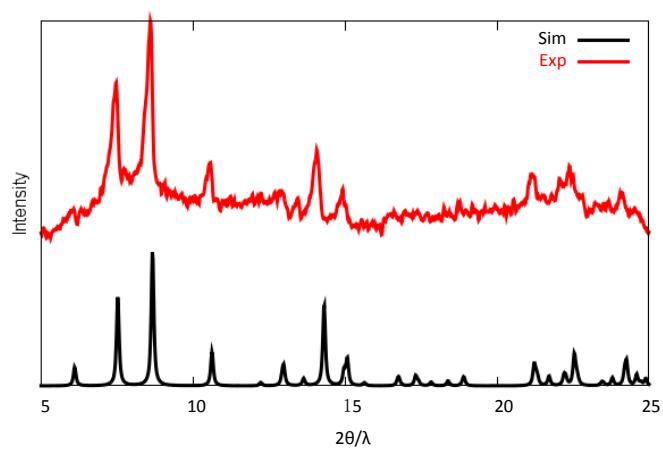


Fig. S18 Experimental (Exp) and simulated (Sim) powder diffraction pattern of **4**.

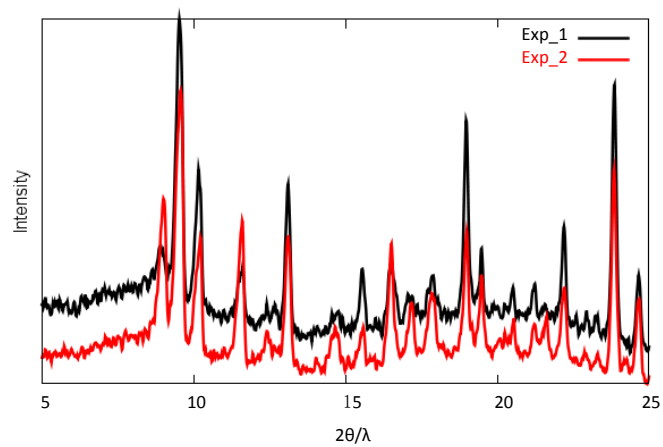


Fig. S19 Two experimental powder diffraction patterns of **5** showing the same solid is obtained reproducibly.

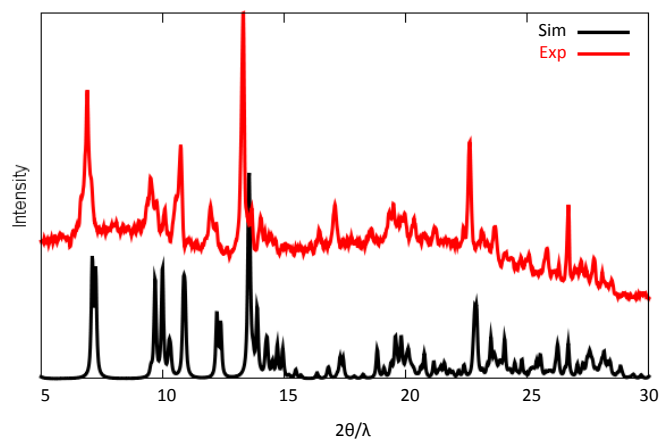


Fig. S20 Experimental (Exp) and simulated (Sim) powder diffraction pattern of **6**.

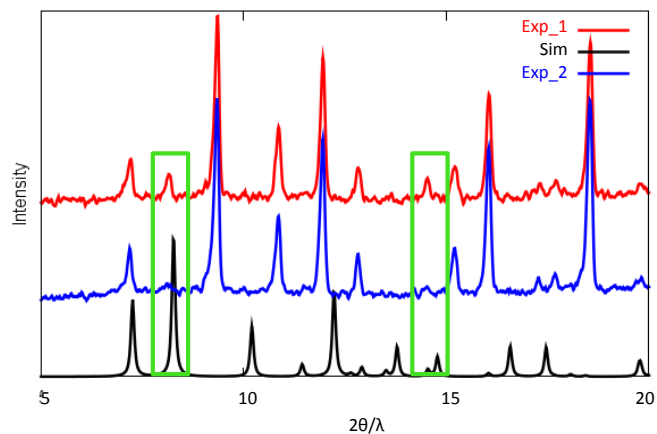


Fig. S21 Simulated (Sim) powder diffraction pattern of **7** based on the single crystal diffraction experiment and two successive experimental powder patterns. Exp1 what obtained after 5 min; diffraction intensities are mostly due to a desolvated product of unknown structure, the regions highlighted in green show residual diffraction intensity due to the original solvate. Exp2 exclusively corresponds to desolvated product.

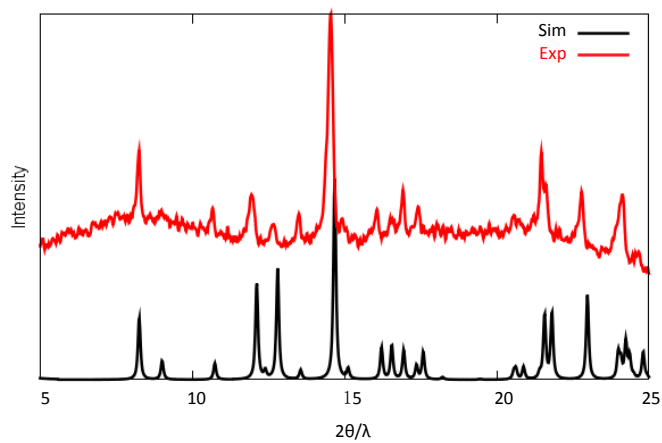


Fig. S22 Experimental (Exp) and simulated (Sim) powder diffraction pattern of **8**.